

APPLICATION OF CONTINUATION METHODS TO THE CALCULATION OF SOLID -FLUID -FLUID AND RELATED SOLID -FLUID EQUILIBRIA OF BINARY ASYMMETRIC MIXTURES IN WIDE RANGES OF CONDITIONS

S.B. Rodriguez-Reartes⁽¹⁾, M. Cismondi⁽²⁾, M.S. Zabaloy^(1,*)

⁽¹⁾PLAPIQUI - Universidad Nacional del Sur – CONICET – CC 717 – 8000 – Bahía Blanca – Argentina.

E-mail: mzabaloy@plapiqui.edu.ar

⁽²⁾Facultad de Ciencias Exactas Físicas y Naturales. Universidad Nacional de Córdoba – Córdoba – Argentina.

The efficient calculation of the global phase equilibrium behavior of asymmetric n-alkane / n-alkane binary mixtures, in wide ranges of conditions, is relevant for understanding wax deposition phenomena. In this work, we propose and explore the use of path-following methods for tracking entire solid-fluid (SF) and solid-fluid-fluid (SFF) equilibrium curves for binary asymmetric mixtures. Our case studies are the highly asymmetric systems: Methane (C_1) / n-Eicosane (C_{20}) [1], Methane (C_1) / n-Tetracosane (C_{24}) [2] and Methane (C_1) / n-Triacontane (C_{30}) [3]. We obtained complete SFF equilibrium lines and SF equilibrium isopleths, isobars and isotherms, in single runs, by using the continuation approach, which makes possible to define robust calculation algorithms. The construction of SF lines takes advantage of information corresponding to SFF lines, generated previously. We also introduce in this work a modeling approach which pays close attention to the limit where the pure heavy component is under solid-liquid equilibrium conditions. The model assumes that the solid phase is only formed by the pure heavy component, and does not consider polymorphic transformations. For describing the fluid phases we use the Peng-Robinson equation of state (PR-EOS). Although the model is relatively simple, it is able to grasp the complex observed behavior for the studied systems.

Keywords: Solid-Fluid Equilibrium, Solid-Fluid-Fluid Equilibrium, Continuation Method, binary n-alkane systems.

INTRODUCTION

Recent technological improvements make possible the exploitation of oil and gas accumulations at very high reservoir depths. In such “hyperbaric” reservoirs the fluid pressure and temperature can reach 2000 bar and 200 °C, respectively ([3], [4]). Hyperbaric reservoir fluids are complex multicomponent mixtures, with a high methane concentration and significant amounts of long chain n-alkanes. The special features of these petroleum reservoirs are the cause of important problems during exploitation, production and transport. One of the major problems is the precipitation of waxes, i.e., the appearance of solid deposits composed of long-chain hydrocarbons. Progress in modelling of wax deposition phenomena requires, as a necessary condition, the study of the global phase equilibrium behavior of asymmetric n-alkane / n-alkane binary mixtures in wide ranges of conditions. Modeling efforts require the availability of robust calculation procedures. In this work, we implemented path-following methods for tracking entire solid-fluid (SF) and solid-fluid-fluid (SFF) equilibrium curves for binary asymmetric systems. Such methods are able to track highly curved lines. The systems

that we studied in this work are Methane (C₁) / n-Eicosane (C₂₀) [1], Methane (C₁) / n-Tetracosane (C₂₄) [2] and Methane (C₁) / n-Triacontane (C₃₀) [3]. In all these systems, a solid-liquid-vapor (SLV) equilibrium line has been experimentally encountered. The SLV curve extends from the pure heavy component triple point to the second critical end point of the mixture (were a single critical fluid phase is in equilibrium with a solid phase). Convergence of conventional calculation algorithms at conditions close to those of the 2nd critical end point is difficult. This justifies exploring the performance of path following (continuation) methods. This is the main purpose of the present work.

MODEL AND CALCULATION ALGORITHMS

In this work, we first deal with the fluid-fluid (FF) equilibrium and then with the solid-fluid (SF) equilibrium. For describing the fluid state, we use the Peng-Robinson (1976) equation of state (PR-EOS). For the systems studied, we fit the PR-EOS interaction parameters [k_{ij} (attractive) and l_{ij} (repulsive)] by reproducing experimental FF equilibrium data, as previously described [5]. The properties of the pure substances and the values of the interaction parameters are reported in Tables 1 and 2 respectively.

Table 1 – Properties of pure substances

Compound	T_{tp}/ K^*	P_{tp}/ Pa^{**}	T_{crit}/ K^*	P_{crit}/ Pa^*	ω^*
Methane	90.694		190.564	4599000	0.0115478
n-Eicosane	309.58	2.10470817E-7	768	1160000	0.906878
n-Tetracosane	323.75	3.20150018E-8	804	980000	1.07102
n-Triacontane	338.65	2.33211307E-9	844	800000	1.30718

* From DIPPR database [6]. T_{crit} = Critical Temperature. P_{crit} = Critical Pressure. ω = Acentric factor.

** P_{tp} = PR-EOS pure compound vapor-liquid equilibrium pressure at the triple point temperature T_{tp} (this work).

Table 2 – Binary interaction parameters for the PR-EOS [5].

System	k_{ij}	l_{ij}	Source of Exp. Data
Methane – n-Eicosane	0.0631	0.0134	van der Kooi et al. (1995), [1]
Methane – n-Tetracosane	0.0596	0.0132	Flöter et al. (1997), [2]
Methane – n-Triacontane	0.0611	0.0206	Machado and de Loos (2004), [3]

For the highly asymmetric systems that we consider here, we assume that the solid phase in any equilibrium situation is composed of only the pure heavy compound. Thus, once we establish an equation for calculating the fugacity of the pure solid as a function of temperature and pressure, we can calculate both, solid-fluid and solid-fluid-fluid equilibria. In this work, we compute SFF equilibria and also isothermal / isobaric / isoplethic SF equilibria, using numerical continuation methods in all cases. Continuation methods are known for their ability to track highly curved lines. Due to space limitations, we describe here our calculation strategy only for the SFF case. For that, we denote the relationship between the absolute temperature (T), the molar volume (V), the composition (z_2 = mole fraction of component 2; label 2 corresponds to the heavy component), and the absolute pressure (P), at fluid state, as $P = h_{pVT}(T, z_2, V)$, where the function h_{pVT} corresponds to the PR-EOS. \hat{f}_i is the fugacity of component “ i ” in a fluid mixture. \hat{f}_i depends on the same variables than function h_{pVT} , i.e., $\hat{f}_i = \hat{f}_i(T, z_2, V)$. This last functional relationship also corresponds in this work to the PR-EOS. The system of equations that we used for calculating the relationship between temperature (T), pressure (P), fluid phase compositions (y_2 and x_1) and phase molar volumes

(V_x and V_y), at solid-fluid-fluid equilibrium conditions, for a binary asymmetric mixture, when assuming the solid phase as made of the pure heavy compound, is the following:

$$\ln(P) = \ln [h_{PVT}(T, 1, V_o)] \quad (1)$$

$$\ln(P) = \ln [h_{PVT}(T, 1-x_1, V_x)] \quad (2)$$

$$\ln(P) = \ln [h_{PVT}(T, y_2, V_y)] \quad (3)$$

$$\ln [\hat{f}_1(T, 1-x_1, V_x)] = \ln [\hat{f}_1(T, y_2, V_y)] \quad (4)$$

$$\ln [\hat{f}_2(T, 1-x_1, V_x)] = \ln [\hat{f}_2(T, y_2, V_y)] \quad (5)$$

$$\ln [f_2^S(P, T, V_o)] = \ln [\hat{f}_2(T, 1-x_1, V_x)] \quad (6)$$

$$g_{spec}(P, T, x_1, y_2, V_x, V_y, V_o) = S_{spec} \quad (7)$$

In the above equations, T and P are the system temperature and pressure; x_1 and V_x are, respectively, the composition (i.e., mole fraction of component 1) and molar volume of the liquid phase; y_2 and V_y are, respectively, the composition (i.e., mole fraction of component 2) and molar volume of the vapour phase; and V_o is the pure heavy component molar volume, in liquid state, at T and P . Besides, $f_2^S(P, T, V_o)$ is the fugacity of the pure heavy component in solid state at system T and P . $f_2^S(P, T, V_o)$ is given by the following equation:

$$f_2^S(P, T, V_o) = \hat{f}_2(T, 1, V_o) \exp(U) \quad (8)$$

The variable U is defined as follows:

$$U = \frac{\Delta V^{S-L}}{RT_{tp}} \left[C_1 \left(1 - \frac{T_{tp}}{T} \right) + C_2 \left(\frac{T_{tp}}{T} - 1 + \ln \left(\frac{T}{T_{tp}} \right) \right) + C_3 \left(\frac{T}{2T_{tp}} - 1 + \frac{T_{tp}}{2T} \right) + \frac{T_{tp}}{T} (P - P_{tp}) \right] \quad (9)$$

In Eq. (9), the constants T_{tp} , P_{tp} (see Table 1), ΔV^{S-L} , C_1 , C_2 and C_3 correspond to the pure heavy component (component 2). ΔV^{S-L} is the solid-liquid molar volume difference ($v_{solid} - v_{liquid}$). Constants C_1 , C_2 and C_3 characterize the pure heavy component solid-liquid equilibrium curve (melting curve). R is the universal gas constant. $\hat{f}_2(T, 1, V_o)$ is the fugacity of the pure heavy component, in liquid state, at system T and P , and it is given in this work by the PR-EOS. We developed Eq. (8) from clear assumptions about the temperature dependency of the solid-liquid heat capacity difference.

We use function $g_{spec}(P, T, x_1, y_2, V_x, V_y, V_o)$ and parameter S_{spec} to make the number of unknowns become equal to the number of equations. For instance for computing the SFF equilibrium at 700 bar, we would set $g_{spec}(P, T, x_1, y_2, V_x, V_y, V_o) = \ln(P)$ and $S_{spec} = \ln(700)$. In other words, when defining the g_{spec} expression together with the S_{spec} value we spend a degree of freedom.

Eqs. (1) to (6) consider that the system pressure P and temperature T are the same for the three phases at equilibrium. Eq. (4) is the isofugacity condition set for the fluid phases, for component 1 (light component). Eqs. (5) and (6) are the isofugacity conditions, concerning the fluid and solid phases, for component 2 (heavy component).

The variables of the system of equations (1) to (7) are the elements of vector X that we define as follows:

$$X^T = [\ln(P), \ln(T), \ln(x_1), \ln(y_2), \ln(V_x), \ln(V_y), \ln(V_o)] \quad (10)$$

The logarithms in the above equation imply a proper scaling of the system variables.

It can be shown that, once we find a solution for the system of Eqs.(1) to (7), we can calculate the sensitivity vector dX/dS_{spec} in a straightforward way, analogous to the one indicated in Refs. [7] and [8]. Vector dX/dS_{spec} is:

$$\left[\frac{dX}{dS_{spec}} \right]^T = \left[\frac{d \ln(P)}{dS_{spec}}, \frac{d \ln(T)}{dS_{spec}}, \frac{d \ln(x_1)}{dS_{spec}}, \frac{d \ln(y_2)}{dS_{spec}}, \frac{d \ln(V_x)}{dS_{spec}}, \frac{d \ln(V_y)}{dS_{spec}}, \frac{d \ln(V_o)}{dS_{spec}} \right] \quad (11)$$

Vector dX/dS_{spec} quantifies the sensitivity of the solution of the system of Eqs. (1) to (7) with respect to parameter S_{spec} . As part of the procedure for calculating the next point in the SLV equilibrium line being built, we use vector dX/dS_{spec} , both, to choose the expression of $g_{spec}(P, T, x_1, y_2, V_x, V_y, V_o)$ and to initialize the variables of vector X (analogously to Refs. [7] and [8]). The present algorithm allows any of the elements of vector X to be equal to $g_{spec}(P, T, x_1, y_2, V_x, V_y, V_o)$, in a given iteration.

The general procedure for calculating an entire SLV line is : [a] find a solution for the system of equations (1) to (7), [b] calculate the sensitivity vector, [c] choose a expression for function $g_{spec}(P, T, x_1, y_2, V_x, V_y, V_o)$ based on the sensitivity vector, [d] set a new value for parameter S_{spec} , [e] predict the new solution from the new S_{spec} value and from the sensitivity vector , [f] go to step [a] so as to find a new point of the SLV line. For solving the system of Equations (1) to (7) we used the full Newton's method, i.e., Newton's method with analytic derivatives.

Notice that, by basically using the same general curve tracking procedure outlined above, it is possible to calculate isothermal, isobaric or isoplethic solid-fluid equilibrium lines. We obtain the corresponding systems of equations by removing some of the equations of the set (1) to (7), and by adding additional constraints, which set the value of temperature, or pressure, or composition of the fluid phase. The construction of SF lines takes advantage of the previously generated SLV line and pure heavy component sublimation and melting lines.

PARAMETERIZATION OF EQ. (8)

For each of the three heavy n-alkanes here considered, we obtained the parameters C_1 , C_2 and C_3 of Eq. (9) by regressing pure compound solid-fluid equilibrium experimental data from Refs.[[1], [2] and [3]]. For each binary system, we fitted ΔV^{S-L} from experimental mixture solid-fluid equilibrium data ([1], [2], [3]). Table 3 reports the values we obtained in this work for C_1 , C_2 , C_3 and ΔV^{S-L} .

In Fig. 1, the curve at unity n-Eicosane mole fraction, shows that the values of C_1 , C_2 and C_3 from Table 3, for n-Eicosane, properly reproduce the pure n-Eicosane melting experimental data. From Figs. 2 and 5 we conclude the same for n-Tetracosane and n-Triacontane, respectively. We have already stressed [[5], [7]] the importance of a good reproduction of the pure compound solid-liquid equilibrium curve, in a wide pressure range, for the precipitating component, when modeling highly asymmetric binary systems.

Table 3 – Constants for Eq. (9) (this work)

Compound	$\Delta V^{S-L} / (m^3/Kmol)$	C_1 / bar	C_2 / bar	C_3 / bar
n-Eicosane	-0.0525476937	-11688.9617	34047.5683	-70535.1757
n-Tetracosane	-0.0565500835	-14213.5004	605153.4382	-591592.5560
n-Triacontane	-0.0757501185	-13127.8951	13201.6315	-41426.7181

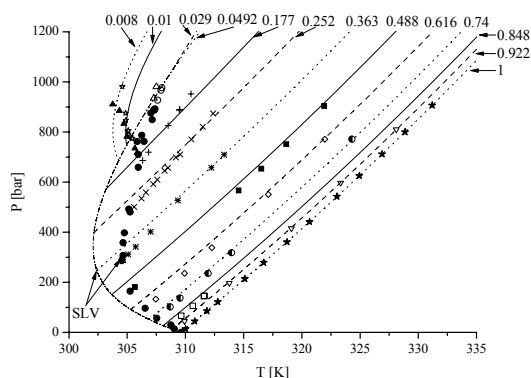


Figure 1 – SF and SFF equilibrium for Methane + n-Eicosane system. Markers: raw isoplethic data [1]: \blacktriangle $x_{C20} = 0.008$, \star $x_{C20} = 0.01$, \triangle $x_{C20} = 0.029$, \circ $x_{C20} = 0.0492$, $+$ $x_{C20} = 0.177$, \times $x_{C20} = 0.252$, $*$ $x_{C20} = 0.363$, \blacksquare $x_{C20} = 0.488$, \diamond $x_{C20} = 0.616$, \bullet $x_{C20} = 0.74$, \square $x_{C20} = 0.848$, ∇ $x_{C20} = 0.922$, \star $x_{C20} = 1$, \bullet SLV equilibrium. Lines: model from this work.

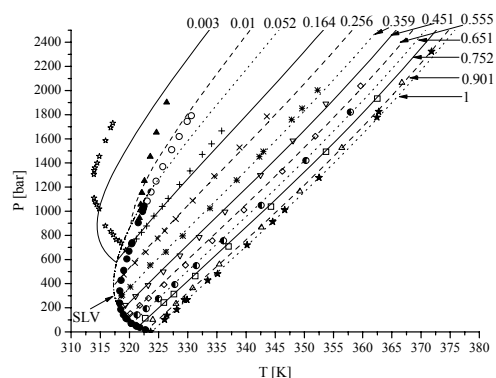


Figure 2 – SF and SFF equilibrium for Methane + n-Tetracosane system. Markers: raw isoplethic data [2]: \star $x_{C24} = 0.003$, \blacktriangle $x_{C24} = 0.01$, \circ $x_{C24} = 0.052$, $+$ $x_{C24} = 0.164$, \times $x_{C24} = 0.256$, $*$ $x_{C24} = 0.359$, ∇ $x_{C24} = 0.451$, \diamond $x_{C24} = 0.555$, \bullet $x_{C24} = 0.651$, \square $x_{C24} = 0.752$, \triangle $x_{C24} = 0.901$, \star $x_{C24} = 1$, \bullet SLV equilibrium. Lines: model from this work.

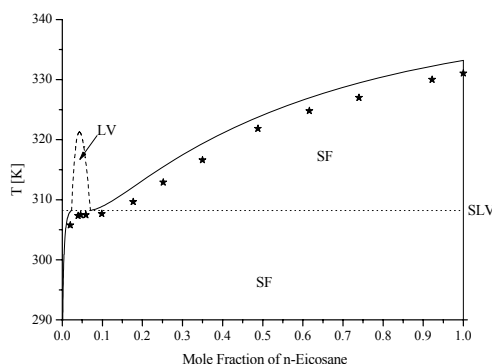
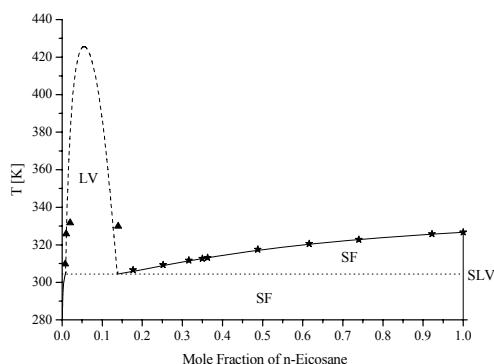


Figure 3 – Phase behaviour for Methane + n-Eicosane system at 700 bar (left) and 1000 bar (right). \blacktriangle VLE and \star SFE experimental data [1] (smoothed in this work). — SFE model (this work), - - - VLE calculated with the PR-EOS and parameters from Table 2 and SLV equilibrium (this work).

RESULTS

From the information in Tables 1, 2 and 3, we calculated SLV equilibrium lines and also isothermal, isobaric and isoplethic Solid-Fluid equilibrium lines. In all cases, our path-following algorithms sequentially constructed entire equilibrium lines, being, each line, generated in a single computer run. The algorithm for the SLV lines showed no convergence problems in the close vicinity of the 2nd critical end point for the three systems considered.

Figures 1, 2 and 5 show, among other calculation results, the model description of the SFF equilibrium curves for the three systems: Methane + n-Eicosane, Methane + n-Tetracosane and Methane + n-Triacontane, respectively. These figures also show SF isopleths for each system. We observe an acceptable agreement between the experimental data and the model.

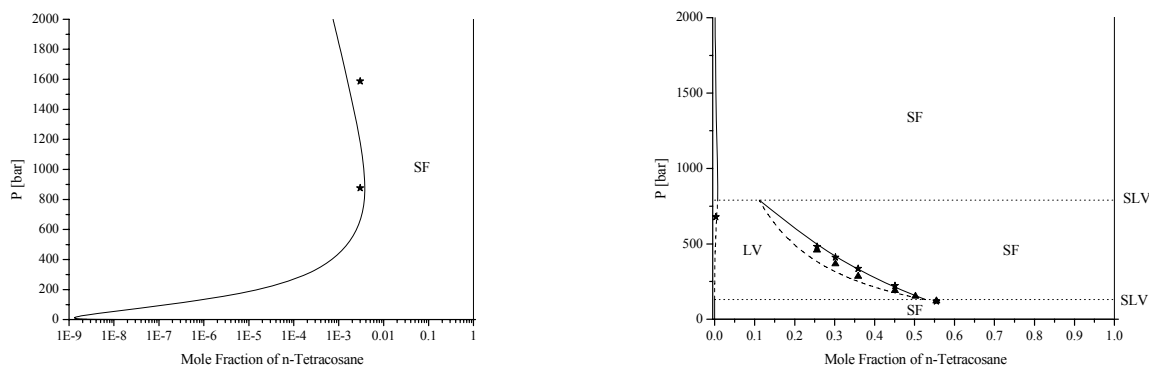


Figure 4 – Phase behaviour for Methane + n-Tetracosane system at 315.9 K (left) and 319.35 K (right). \blacktriangle VLE and \star SFE experimental data [2] (smoothed in this work). — SFE model (this work), - - - VLE calculated with the PR-EOS and parameters from Table 2 and \cdots SLV equilibrium (this work).

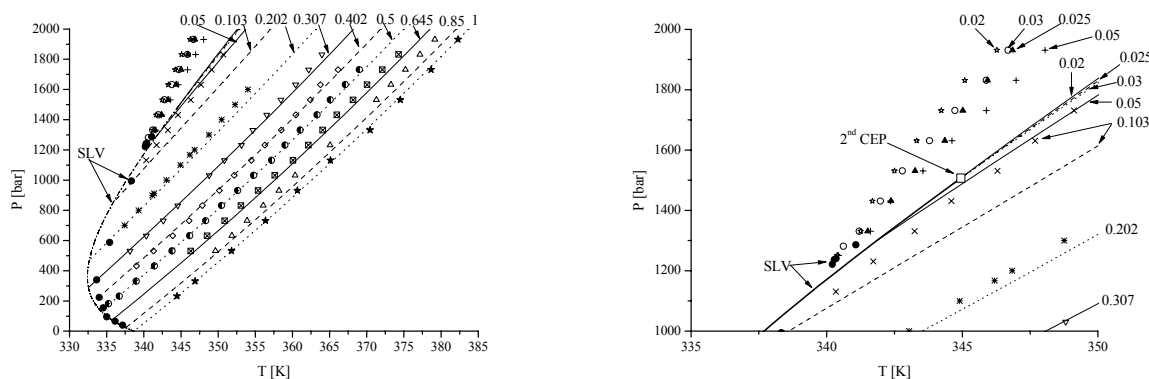


Figure 5 – SF and SFF equilibrium for Methane + n-Triacontane system. Markers: raw isopleth data [3]: \star $x_{C30} = 0.020$, \blacktriangle $x_{C30} = 0.025$, \circ $x_{C30} = 0.030$, $+$ $x_{C30} = 0.050$, \times $x_{C30} = 0.103$, \ast $x_{C30} = 0.202$, ∇ $x_{C30} = 0.307$, \diamond $x_{C30} = 0.402$, \bullet $x_{C30} = 0.5$, \boxtimes $x_{C30} = 0.645$, \triangle $x_{C30} = 0.85$, \star $x_{C30} = 1$, \bullet SLV equilibrium. Lines: model from this work. Right chart: Zoom of the higher Methane concentration portion of the left chart. \square Second Critical End Point (model).

Figure 3 depicts Txy projections (isobars) for Methane + n-Eicosane system. Figures 4 and 6 show Pxy projections (isotherms) for Methane + n-Tetracosane and Methane + n-Triacontane systems respectively. Notice that figs. 3, 4 and 6 show both, equilibria involving a solid phase and also equilibria involving only fluid phases [[9], [10]].

REMARKS AND CONCLUSIONS

In this work, we propose robust algorithms to construct entire solid-fluid (SFE) and solid-fluid-fluid (SFFE) equilibrium curves for binary n-alkane asymmetric mixtures. The algorithms make use of numerical continuation methods. Such methods take advantage of the information contained within the sensitivity vector (dX/dS_{spec}) to efficiently track non linear

equilibrium curves. We have found that our algorithms have a very good performance. For the SLV lines, there were no convergence problems in the vicinity of the 2nd critical end point. For SF lines, our algorithms were able to track lines of widely variable shape. We also propose here a modeling approach which, by construction, guarantees a good model performance at high concentration for the heavy component. With regard to the model parameterization, we have avoided in this work the simultaneous matching of solid-fluid and fluid-fluid equilibrium data, i.e., we first deal with the FFE problem and then with the SFE problem. In view of the simplicity of the model, we conclude that the agreement between the model and the experimental data is good. There is still room for improvement. A road that may lead to such improvement could be the use of mixing rules more suited for asymmetric systems, within the fluid phase equation of state.

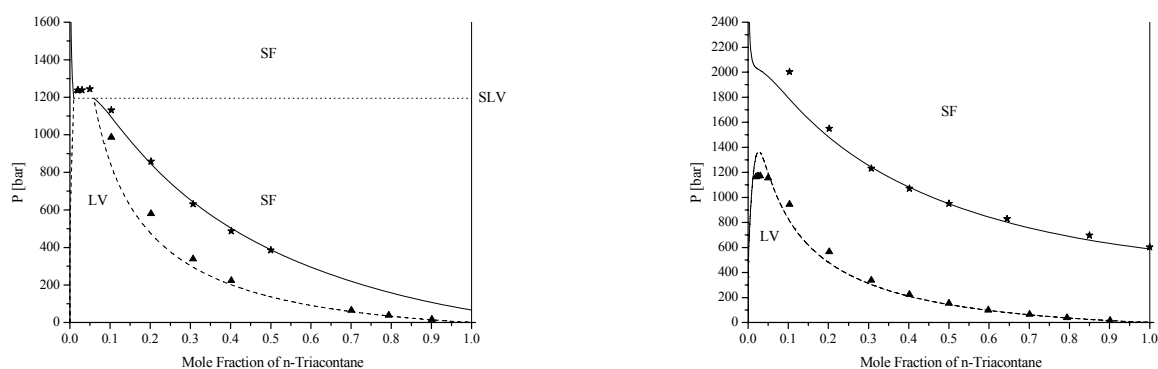


Figure 6 – Phase behaviour for Methane + n-Triacontane system at 340.34 K (left) and 353.15 K (right). \blacktriangle VLE and \star SFE experimental data [3] (smoothed in this work). — SFE model (this work), - - - VLE calculated with the PR-EOS and parameters from Table 2 and \cdots SLV equilibrium (this work).

REFERENCES

- [1] VAN DER KOOIJ, H.J., FLÖTER, E., DE LOOS, TH.W., *J. Chem. Thermodyn.*, Vol. 27, **1995**, p. 847.
- [2] FLÖTER, E., DE LOOS, TH.W., DE SWAAN ARONS, J., *Fluid Phase Equilib.*, Vol. 127, **1997**, p. 129.
- [3] MACHADO, J.J.B., DE LOOS, TH.W., *Fluid Phase Equilib.*, Vol. 222–223, **2004**, pp. 261–267.
- [4] MACHADO J.J.B., DE LOOS TH.W., *Fluid Phase Equilib.* Vol. 226, **2004**, p. 83.
- [5] RODRIGUEZ-REARTES, S.B, CISMONTI, M., ZABALOY, M.S. “Modelling The High Pressure Solid-Fluid Equilibrium In Asymmetric Systems”. I Conferencia Iberoamericana de Fluidos Supercríticos PROSCIBA 2007. Foz de Iguazú-Brasil, 10 al 13 de abril de **2007**. Trabajo (SC-48).
- [6] DIPPR 801, Evaluated Process Design Data, Public Release (**2003**), American Institute of Chemical Engineers, Design Institute for Physical Property Data, BYU-DIPPR, Thermophysical Properties Laboratory. Provo, Utah.
- [7] S.B. RODRIGUEZ-REARTES, M. CISMONTI, M.S. ZABALOY. “Numerical Continuation Method For High Pressure Solid-Fluid Equilibrium Calculations In Asymmetric Systems”. 23rd European Symposium on Applied Thermodynamics. (Cannes-France, May 29 to June 1st, **2008**). Work (PII-57).
- [8] CISMONTI, M., MICHELSEN, M. L., *J of Supercritical Fluids*. Vol. 39, **2007**, pp. 287-295.
- [9] CISMONTI, M., NUÑEZ, D.N., ZABALOY, M.S., BRIGNOLE, E.A., MICHELSEN, M.L., MOLLERUP, J.M. GPEC: A Program for Global Phase Equilibrium Calculations in Binary Systems. EQUIFASE 2006: VII Conferencia Iberoamericana sobre Equilibrio entre Fases para el Diseño de Procesos. Morelia, Michoacán, México. October 21-25, **2006**. Full paper available in EQUIFASE 2006 CD-ROM.
- [10] CISMONTI, M., MICHELSEN, M. L., ZABALOY, M.S. "Automated Generation of Phase Diagrams for Supercritical Fluids from Equations of State". (oral presentation) 11th European Meeting on Supercritical Fluids" (Barcelona-Spain, May 4- 7, **2008**).